Biomaterials Science

Insight into the efficient transfection activity of a designed low aggregated magnetic polyethyleneimine/DNA complexes in serum-containing medium and the application in vivo

Journal:	*Biomaterials Science*
Manuscript ID:	BM-ART-08-2014-000317.R2
Article Type:	Paper
Date Submitted by the Author:	12-Oct-2014

Complete List of Authors:	Xie, Li; National Engineering Research Center for Biomaterials, Jiang, Qian; National Engineering Research Center for Biomaterials, He, Yiyan; National Engineering Research Center for Biomaterials, Nie, Yu; Sichuan University, National Engineering Research Center for Biomaterials Yue, Dong; National Engineering Research Center for Biomaterials, Gu, Zhongwei; National Engineering Research Center for Biomaterials,

Biomaterials Science

RSCPublishing

ARTICLE

Insight into the efficient transfection activity of a designed low aggregated magnetic polyethyleneimine/DNA complexes in serum-containing medium and the application *in vivo*

Cite this: DOI: 10.1039/x0xx00000x

Received 00th January 2014,
Accepted 00th January 2014

DOI: 10.1039/x0xx00000x

www.rsc.org/

Li Xie, Qian Jiang, Yiyan He, Yu Nie*, Dong Yue, Zhongwei Gu*

A designed low aggregated magnetic polyethyleneimine/DNA (MPD-cc) complexes showed efficient transfection in serum-containing medium for PEI-mediated gene transfection *in vitro* and *in vivo*, but the mechanism remains unclear. The present study provided an insight into the extracellular and intracellular fates of the magnetic gene complexes, evaluated their transfection efficiency and body distribution after systemic administration assisted by fluorescent imaging technology. The PEI cationic complexes in our study switched to be negatively charged in the serum-containing medium due to protein corona formation, and the complexes displayed negligible aggregation from transmission electron microscopy observation and dynamic light scattering analysis. However, the SDS-polyacrylamide gel electrophoresis (SDS-PAGE) showed that less protein was adsorbed on magnetic gene complexes during a 10-min magnetofection compared with that associated with traditional polyethyleneimine/DNA (PD) complexes after a long-term (4 h) incubation. In terms of cellular uptake and internalization evaluation by flow cytometry, magnetofection with our designed MPD-cc complexes showed obvious superiority in the presence of serum than traditional transfection (PD complexes). Moreover, confocal laser scanning microscopy revealed that after internalization, fewer MPD-cc in magnetofection were trapped in endosome, while more were found in nucleus than PD and MPD-cc without magnetic field. Putting these facts together, we conclude that magnetofection by the designed MPD-cc complexes facilitates many processes of transfection, including less protein adsorption, efficient cellular sedimentation and internalization, as well as endosomal escape and nuclear import. In the near infrared imaging study, it was observed that the accumulation of complexes in tumor by magnetic capture was enhanced *in vivo*. All of these improved *in vitro* and *in vivo* functions contributed to a 5-fold enhancement in magnetofection via intravenous delivery.

1. Introduction

Non-viral vectors for gene delivery have gained increasing attention for both clinical and basic science research because of the clear advantages over viral vectors, such as low immunogenicity, good biocompatibility, large DNA loading capacity, as well as controllable synthesis and modification[1, 2]. Cationic carriers, especially the benchmark polyethyleneimine (PEI), can effectively package DNA into nano-scaled complexes via electrostatic attraction, and are widely used for *in vitro* gene delivery. However, once applied in simulated physiological environment or *in vivo*, polyethyleneimine and its derivatives suffer from the serious problem of serum protein interference, leading to a sharp drop in transfection efficiency with serum and lack of targeting *in vivo*.

Various chemical and biological strategies have been applied to overcome the inhibitory impact of serum, such optimization of the charge ratio[3], application of negatively charged coating[4] and PEG modification[5]. Targeting ligands, antibodies or peptides are conjugated to PEI for the improvement in site-specific gene delivery[3, 6]. Besides these efforts, some physical techniques such as magnetofection showed to promisingly reserve the transfection efficiency under serum conditions[7-10], and achieve magnetic field guided site-specific accumulation via local injection[11].

However, most PEI-containing magnetic particles formed large aggregates especially after they are complexed with DNA (> 600 nm), the large size would reduce the transfection activity of magnetic polyethyleneimine/DNA complexes in serum-containing medium and restrict their application *in vivo* due to fast clearance by the reticuloendothelial system[12]. Thus, improvements in the preparation of less aggregated magnetic particles were reported recently, by adjusting the mixture ratio of PEI to magnetic particles[13, 14], deaggregation by acidification[13] or by applying a stabilizing coat[15]. In our previous study, a designed MNP-cc/PEI/DNA complexes (MPD-cc) were prepared by mixing

carboxylic acid-silane coated magnetic particles and PEI/DNA complexes with low aggregated size (< 150 nm) and high magnetic response ability (50 emu/g particles) (Scheme 1)[10]. Even these complexes have exhibited 3 orders of magnitude higher transfection efficiency *in vitro* and 15-fold magnetofection efficiency *in vivo* by intratumoral injection, the exact processes of transfection remain to be defined.

The possible mechanisms of various magnetofection are under intensive investigation in recent years without final conclusion. Some researchers found that the major advantages of magnetofection were not from cellular uptake pathway or internalization dynamics, but only lied in an accelerated sedimentation of complexes on the cell surface driven by the magnetic field[16, 17]. While others revealed that the assembly sequence, surface property and charge of magnetic vector could affect the intracellular process and location, leading to different transfection efficiency[18]. Many studies on non-magnetic gene delivery system proved that the non-specific adsorption of negatively charged proteins has strong association with serum-triggered transfection inhibition[8, 9]. Inspired by these results, we want to go insight into the details of magnetofetion including protein corona, intracellular location and nucleus transportation (Scheme 1).

Moreover, for the *in vivo* application, high magnetofection efficiency is usually achieved by the direct local injection of complexes into target or surrounding tissues[7, 10, 19]. Many target tissues, such as metastatic tumor nodules, can not be approached by local injection but only through systemic blood circulation. Compared to local administration, systemic application is still a challenge for magnetofection[3]. It is critical that the complexes remain stable exploring to blood components, and are not trapped into other non-target tissues before the target cells can be reached.

So in the present study, our designed magnetic complexes were evaluated for their potential application in the context of systemic administration (Scheme 1). All experiments for magnetic gene complexes characterization and magnetofection activity evaluation were performed in the presence of serum. Protein corona formed on the surface of complexes was analyzed by SDS-PAGE, and intracellular location was monitored with the assistance from fluorescent labeled complexes. Magnetofection efficiency and near infrared imaging of magnetic gene complexes were assessed after intravenous injection.

2 Experimental section

2.1 Materials

Branched polyethyleneimine (PEI, Mw 25 kDa), Dulbecco's modified Eagle's medium with high glucose (DMEM) and fetal bovine serum (FBS) were obtained from Life Technologies Corporation (Gibco®, USA). Antibiotics (penicillin & streptomycin) and fluorescein isothiocyanate (FITC) were obtained from Sigma (USA). pEGFP encoding green fluorescent protein (GFP) and pGL3 encoding luciferase were purified with EndoFree Plasmid Kit from Qiagen (Germany). Plasmid pCMV-Luc was constructed by cloning the luciferase gene from pGL3 promoter vector into pcDNA3.1 and purified with EndoFree Plasmid Kit from Qiagen. Human hepatoma cell line (HepG2) was obtained from Shanghai Institutes for Biological Sciences (China). Nucleic acid labeling kit Label IT®Cy5™ was from Mirus Bio Corporation (USA). N-(trimethoxysilylpropyl) ethylenediaminetriacetic acid (45% in water) (carboxylic acid-silane) was obtained from ABCR GmbH (Germany). Coomassie brilliant blue G-250 was purchased from Sigma-Aldrich (USA). Lysotracker® Blue DND-22 was obtained from Introgen (USA). DAPI was bought from Beyotime (China). All buffers were prepared in MilliQ ultrapure water and filtered (0.22 μm) prior to use, and all the other chemicals were purchased from Kelong Chemical Co (Chengdu, China) and used without further purification.

2.2 De novo synthesis of magnetic nanoparticles and preparation of gene complexes

The magnetic particles used for gene complexes assembly were synthesized by chemical coprecipitation method and further modified by carboxylic acid-silane according to our previous study[10], called MNP-cc. The obtained MNP-cc showed spherical shape with

Biomaterials Science

RSCPublishing

ARTICLE

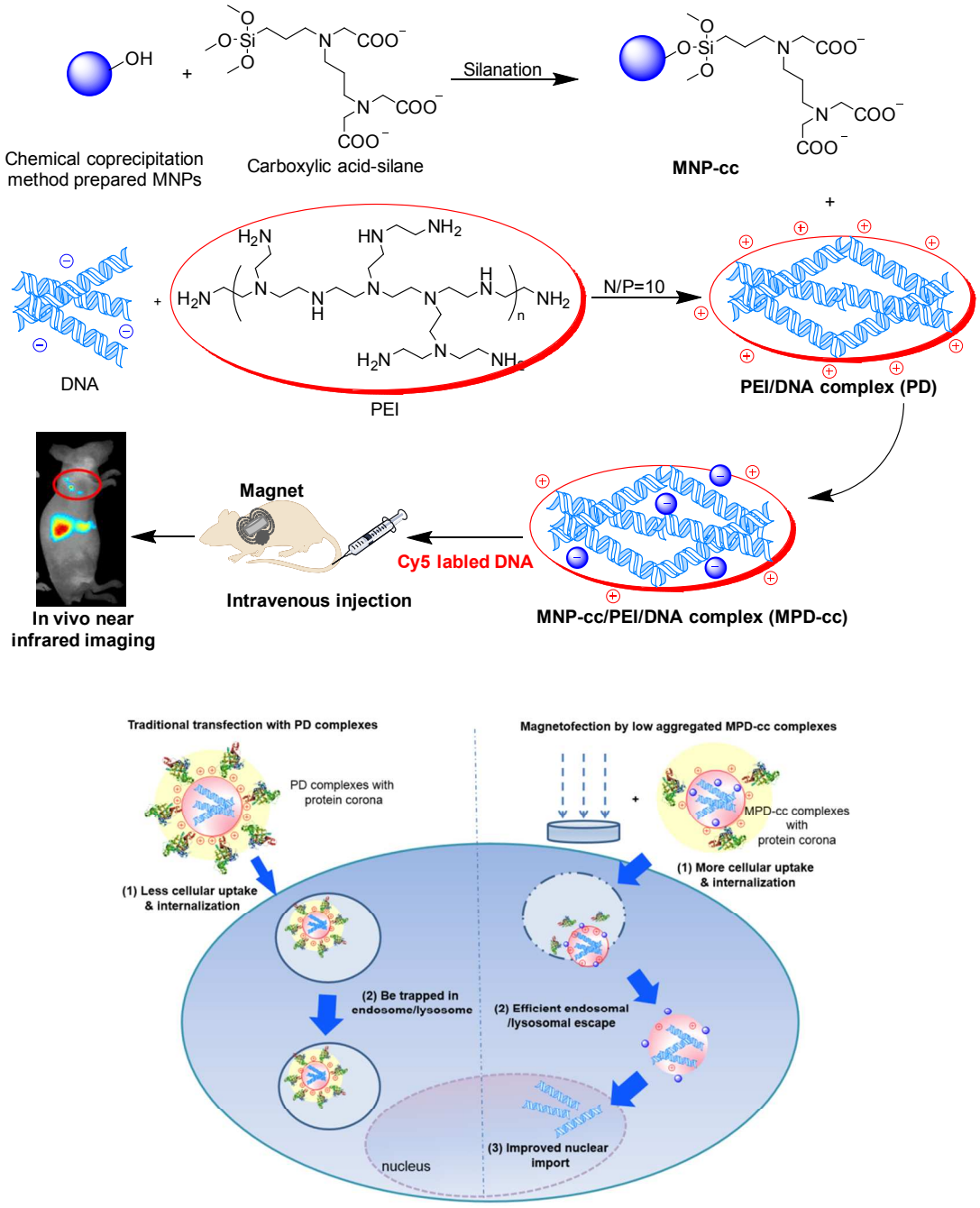

Scheme 1 Schematic representation of the *in vitro* and *in vivo* applications of gene complexes

hydrodynamic diameter of ~ 25 nm and zeta potential of ~ -26 mV by Malvern instrument of Zetasizer Nano ZS. The saturation magnetization of superparamagnetic MNP-cc was 50 emu/g particles.

Magnetic gene complexes composed of plasmid DNA, PEI, and MNP-cc were prepared by electrostatic interaction to form the ternary components in sequence (Scheme 1)[10]. DNA, PEI and MNP-cc were diluted in HBG buffer (HEPES 20 mM, pH 7.4, 5% glucose), separately. The PEI/DNA binary complexes (PD) were formed at PEI nitrogen to DNA phosphate (N/P) ratio of 10, and MNP-cc/PEI/DNA complexes (MPD-cc) were fabricated by adding MNP-cc to the pre-prepared PD complexes at metal (Fe) to DNA

weight ratio of 0.4 or 0.8. All gene complexes were characterized by size and zeta potential in the serum-containing conditions at a final DNA concentration of 3 μg/mL by Zetasizer Nano ZS (Malvern Instruments, Worcestershire, UK). Before the measurement, gene complexes were mixed with an equal volume of 20% serum-containing DMEM for 10 min or 4 h, and diluted with water to a final volume of 1 mL. The morphology of MPD-cc was observed by transmission electron microscopy (TEM, JEM-100CX, JEOL, Japan).

2.3 Gene transfection *in vitro*

HepG2 cells were maintained in the DMEM culture medium containing 10% FBS, 100 μg/mL streptomycin and 100 IU/mL penicillin at 37°C in a humidity atmosphere of 5% CO_2 incubator. Cells were seeded into 6-well plate at a density of 2×10^5 cells per well and cultured for 24 h. Prior to transfection, the medium was replaced with 90 μL fresh culture medium with 10% FBS. 10 μL of PD or MPD-cc complexes were then added to achieve a final DNA concentration of 2 μg/mL (100 μL of medium/well) and incubated for 10-min or 4-h time period.

In magnetic assisted transfection (magnetofection), an array of 6 neodymium-iron-boron (Nd-Fe-B) permanent magnets (d = 30 mm, h = 10 mm; Shenzhen LiHeng Magnet Company, China) in the format of a 6-well plate was placed under the cell culture plate to offer 120 mT magnetic field. After 10 min incubation, magnetic field was removed and the medium was replaced by 2 mL of fresh culture medium. The expression of green fluorescent protein was first observed by an inverted fluorescence microscope (Leica, Germany) when the continued incubation time reached to 48 hours. Cells were subsequently washed with PBS, harvested with trypsin treatment and collected in 2% FBS-containing PBS. The gene transfection efficiency was then quantified using flow cytometry (BD FACSAria™ II, Franklin Lakes, NJ) by measuring the percentage of GFP-positive cells in 1×10^4 gated events per sample.

2.4 SDS-PAGE analysis of protein adsorption on gene complexes

PD and MPD-cc complexes (with 2 μg pEGFP) were incubated with 1 mL of 10% FBS-containing DMEM medium for 10 min or 4 h under 120 mT magnetic field to imitate magnetofection or kept untreated. After incubation, the samples were centrifuged (15 min at 12,000 rpm at 4°C) to pellet the gene complexes and adsorbed serum proteins (protein corona) which were separated from the supernatant medium. The pellet was then resuspended in 500 μL of PBS and was extensively washed with cold PBS thrice. Immediately after the last washing step the MPD-cc/protein corona pellet was mixed with protein loading buffer [250 mM Tris-HCl pH 6.8, 10% (w/v) SDS, 50% (v/v) glycerol, 5% (v/v) DTT and 0.05% (w/v) bromophenol blue], boiled for 5 min at 100°C, and loaded on 10% polyacrylamide gel for electrophoresis at 120 volt until the loading buffer completely ran out from the gel. After stained with coomassie blue dye and washed with deionized water, the gel was scanned and imaged using a Biorad GS-800 calibrated densitometer scanner (Bio-Rad, USA). The experiment was conducted for at least three independent samples and performed in triplicates to ensure reproducibility of the gene complexes/serum protein pellet sizes, general pattern, and band intensities on the SDS-PAGE gel.

2.5 Electrochemical impedance measurement

Electrochemical impedance spectroscopy (EIS) method was performed for the evaluation of cell membrane integrity using a Gamry Reference 600 Potentiostat (Gamry instruments, Warminster, PA, USA), over a frequency range from 10 Hz to 1 MHz with 5 mV amplitude of sinusoidal voltage. The electrodes for detection were self-made stainless steel ones with well biocompatibility and highly polarity. The cell-device system for electrochemical impedance measurements was assembled as described in Fig. S1. Two electrodes were installed inside the transwell unit with 0.4 μm pore size (Millipore, Cambridge, MA, USA) and the outer chamber of 24-well culture plate, respectively.

The transwell support was coated with cells 48 h earlier to obtain the integral monolayer without further increase in the impedance and with the lowest deviation of the impedance signals[20]. The same concentration of MNP-cc or PD complexes as transfection *in vitro* was added for 4 h incubation, while MPD-cc complexes were incubated with cells for 10 min with magnetic field as the transfection process described in the section "2.3. Gene transfection *in vitro*". Four or twenty-four hours post incubation, the impedance signals were recorded at 10 kHz frequency which showed the highest sensitivity[21]. All of the recorded impedance data were processed with EIS300 Software. The relative impedance magnitude values of cells treated with gene complexes were calculated against control cells with HBG buffer. In order to remove the disturbance of magnetic field, the measurement of impedance magnitude was carried out with/without exposure to magnetic field. In addition, the changes of cell membrane capacitance were deduced from the impedance spectra by the equation in Kurzweil's study[22]. They were monitored from the beginning of gene complexes added to cells till 90 min when the capacitance achieved a plateau in a real-time model. 300 kHz frequency was selected for the measurement since the maximum capacitance change was achieved.

2.6 Cellular uptake and internalization by flow cytometry

HepG2 cells were seeded at a density of 3×10^5 cells per well in 6-well plate and incubated overnight for attachment. The medium was replaced with fresh culture medium containing complexes (formulated with FITC labeled PEI[23]) at a final DNA amount of 2 μg/mL. Three kinds of incubation modes with gene complexes were used: (Ⅰ) 10 min incubation, (Ⅱ) 4 h incubation, (Ⅲ) 10 min incubation, washing with cold PBS and another 4 h incubation with fresh culture medium (10 min + W + 4 h). Magnetic field of 120 mT was applied for the 10-min incubation with MPD-cc complexes. At the indicated time points, cells were washed twice, harvested by trypsin treatment and finally gathered in 2% FBS containing ice-cold PBS for flow cytometry monitor. In the case of cell internalization studies, trypan blue was added at a final concentration of 0.4% to quench the extracellular but not the intracellular fluorescence of FITC[17]. To obtain the intuitive view of the differences, the confocal microscopy images were taken and shown in Fig. S2.

2.7 Intracellular fate of magnetic complexes by confocal laser scanning microscopy

Cells were seeded at a density of 2×10^4 cells per well in a 35 × 12 mm glass-bottomed chamber (NEST, China). Complexes of PD and MPD-cc containing FITC labeled PEI and 40% Cy5 labeled pGL3 were added into serum-containing culture medium to a final quantity of plasmid DNA of 300 ng per chamber. Incubation with 120 mT

extra-magnetic field for 10 min was applied to mimic the magnetofection, followed by refreshment of medium for further culture. The intracellular behavior of gene complexes was monitored using confocal laser scanning microscope (CLSM, Leica TCS SP5, Germany) at 4 and 24 h after the addition of the fluorescent complexes. Twenty minutes prior to the observation, the lysosomes were stained by 75 nM of lysoTracker™ DND-22. To visualize the nucleus, the cells were fixed with 4% paraformaldehyde and stained with DAPI for 5 min. The Cy5 fluorophore was excited at 633 nm and the emission was detected with a 650 - 750 nm band pass filter. FITC was excited at 488 nm and the emission was detected with a 500 - 550 nm band pass filter. LysoTracker™ DND-22 and DAPI were excited at 405 nm and the emission was detected with a 422 nm band pass filter.

2.8 *In vivo* trafficking gene complexes and gene transfection evaluation

All animal experiments were performed in accordance to our institutional and NIH guidelines for care and use of research animals. BABL/c nude mice with body weight of 19-21 g (Jianyang Experimental Animal Centre, China) were used to create subcutaneous tumors by armpit injecting HepG2 cells (1×10^6 cells per mouse) into mice. Various gene complexes (PD or MPD-cc) containing Cy5 labeled pGL3 were injected into the tail vein of mice at a dose of 50 μg DNA/mouse when tumor reached a diameter of ~ 8 mm. For the magnetofection, externally applied magnetic field (Nd-Fe-B magnet, d = 10 mm, h = 6 mm, with magnetic remanence of 400 mT) was fixed over the surface of tumor before the administration, and remained until desired time for *in vivo* near infrared imaging (NIR). Untreated mice were used as control. At 8 h post administration, the mice were anaesthetized with 5% chloral hydrate and visualized using a CRI Maestro Imaging System (Cambridge Research & Instrumentation, Inc., USA). Fluorescence images were captured by illumination with a halogen lamp using an appropriate filter combination (excitation filter 607 nm, emission filter 670 nm). After the last imaging session, mice were sacrificed, and the major organs and tumors were separated out to for the NIR evaluation. All fluorescence images were handled with CRI Maestro EX 3.0 analysis software.

Another 24 tumor-bearing mice were randomly divided into four groups (n = 6). 200 μL of PD or MPD-cc complexes containing 50 μg pCMV-Luc was injected via the tail vein. Control group was treated with a same volume of 5% w/v glucose solution. Externally applied magnetic field was fixed over the surface of tumor before injection and remained until mice were sacrificed 48 h later. The tumors and major organs were removed and homogenized with lysis buffer. Supernatant was collected by centrifugation (12,000 rpm/min, 10 min) for the measurements of luciferase activity and protein content. Relative light units (RLU) were measured using the luciferase reporter gene assay kit and a chemiluminometer (Bio-Rad, Model 550, USA), while the total protein content was measured using a BCA protein assay kit and a microplate reader (Bio-Rad, Model 550, USA). Transfection efficiency was expressed as RLU per mg protein.

2.9 Statistical Analysis

All biological data were expressed as means with standard deviations (± S. D.). Statistical analysis was determined by the single factor ANOVA test. Data sets were compared using two-tailed, unpaired t-tests. Values of $p < 0.05$ were considered to be statistically significant.

3 Results and Discussion

3.1 Size and zeta potential of gene complexes

The sizes of PD and MPD-cc complexes were lower than 150 nm with zeta potentials around + 25.1 ~ + 28.8 mV in water, and the diameters were slightly decreased after addition of MNPs (Table 1 and Fig. 1A)[10]. After 10 min or 4 h incubation in the serum-containing medium, the sizes of all gene complexes became larger (~ 220 nm) due to adsorption of negatively charged proteins[24] and formation of protein corona on the surface of particles[25]. Despite the moderately increased particle size, the gene complexes did not show large-size aggregation (Fig. 1B), consistent with the stabilization properties of protein corona found in previous study[26]. The significant change of zeta potential of MPD-cc complexes from positive to negative (~ -11 mV) also confirmed the serum protein adsorption[26]. In simulated physiological or *in vivo* environment, serum protein is considered as the major species that interacts with gene carriers and consequently alters the stability of carriers[27]. In view of this conception, the well distribution of nanocarriers would most likely benefit for the efficient delivery *in vivo*[28].

Table 1 Size and zeta potential of PD and MPD-cc in water and serum-containing DMEM medium

Sample	water		Incubation with serum-containing DMEM medium		
	Size (nm)	Zeta potential (mV)	Incubation time	Size (nm)	Zeta potential (mV)
PD	145.1 ± 4.6	28.8 ± 0.4	4 h	229.0 ± 6.2	-10.6 ± 0.4
			10 min	224.7 ± 7.4	-11.5 ± 0.6
MPD-cc[a]	121.4 ± 2.7	25.1 ± 1.5	10 min	215.6 ± 8.9	-11.0 ± 0.7

[a] MPD-cc at Fe to DNA weight ratio of 0.4.

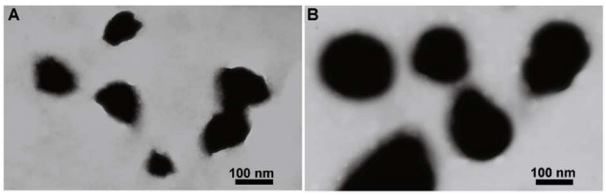

Fig. 1 Transmission electron microscopy (TEM) images of MPD-cc complexes before (A) and after incubation with DMEM containing serum (B). Weight ratio of Fe to DNA in MPD-cc complexes was 0.4. Phosphomolybdic acid was used as a dye. (MPD-cc: MNP-cc/PEI/DNA)

3.2 Gene expression *in vitro*

The expression efficiency of green fluorescent protein (GFP) was evaluated on hepatoma cell line in the presence of serum (Fig. 2). After 4 h-incubation, cells in the PD and MPD-cc groups showed fragmentary green fluorescent spots, while the GFP expression intensity was the highest after magnetofection with MPD-cc complexes for 10 min (Fig. 2A). Meanwhile, the percentage of GFP-expressing cells was assessed by flow cytometry (Fig. 2B). Consistent results were obtained that the cells treated with magnetofection showed the highest percentage of GFP-positive cells (11.3%), whereas the value was only 0.5% and 0.7% for the cells

treated with PD and MPD-cc complexes without aid of magnetic field, respectively. The ratios increased slightly to 1.2% and 1.8% respectively with longer treatment (4 h), indicating that extension of the incubation time could not improve transfection by PD and MPD-cc without magnetic field under serum conditions. The superiority of magnetofection described above was in agreement with the results from our previous study by luciferase reporter gene, reconfirming the well serum-tolerant capacity (no statistical difference in transfection either in the presence or absence of serum)[10].

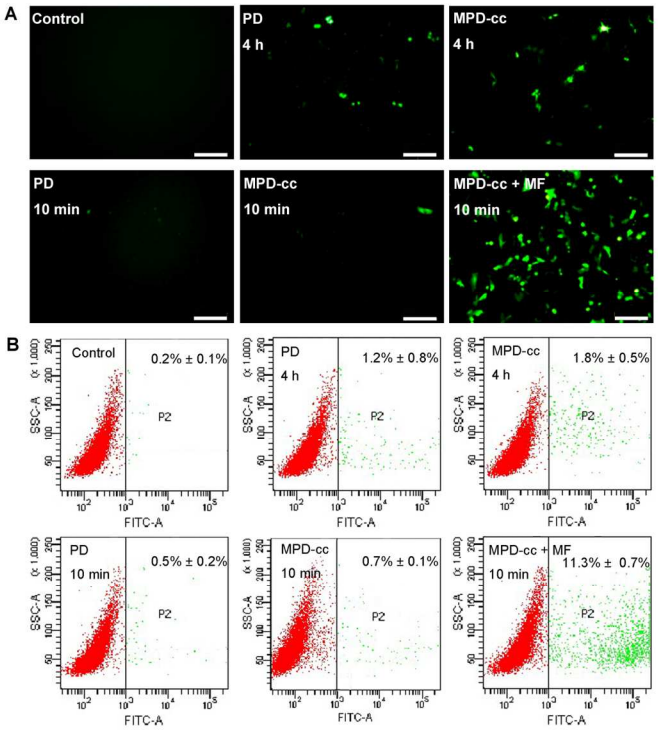

Fig. 2 *In vitro* gene expression on HepG2 cells in the presence of serum. (A) Representative fluorescence microscopy images of green fluorescent protein expression (scale bars = 200 μm). (B) Quantitative evaluation of the percentage of transfected cells by flow cytometry analysis. The values represent as means ± S.D. (n = 5). Magnetofection of MPD-cc complexes was performed with 10-min incubation under external 120 mT magnetic field (MPD-cc + MF). PD and MPD-cc complexes without magnetic field were carried out with 10-min or 4-h incubation. (PD: PEI/DNA, MF: magnetic field)

3.3 Serum protein adsorption on gene complexes

The type and amount of adsorbed proteins (protein corona) were reported to exert diverse effects on the interaction between particles and cells, especially *in vivo*[29, 30]. Thus, the significant difference in gene delivery efficiency between magnetofection and traditional transfection in serum-containing medium provides the impetus to evaluate the serum protein adsorption before complexes entry into cells. The loose protein corona was removed by extensive washing, while bound proteins (the hard corona) were assayed by 10% SDS-PAGE gel (Fig. 3)[31, 32]. It was clear that the protein corona of PD and MPD-cc complexes displayed almost the same typical bands with main molecular weight of 70-50 kDa, indicating a similar protein composition. While, the intensity of the bands differed significantly between the two groups. With 10-min incubation, the intensity of typical bands (mainly in albumin of 68 kDa) in magnetofetion condition (MPD-cc + MF) was stronger than that of PD complexes and MPD-cc complexes without magnetic field[33]. After longer incubation (4 h), the amount of absorbed protein was obviously increased, which was a common phenomenon that the hard corona layer increases and the ratio of each component changes with the time, reaching equilibrium at some time point[31, 32, 34]. Thus, shortening the time of interaction with serum (as magnetofection) might be an effective way to decrease the unexpected adsorption of protein[34]. In addition, introduction of MNPs into the PD complexes might bring slight changes in particle size, shape, surface charge and

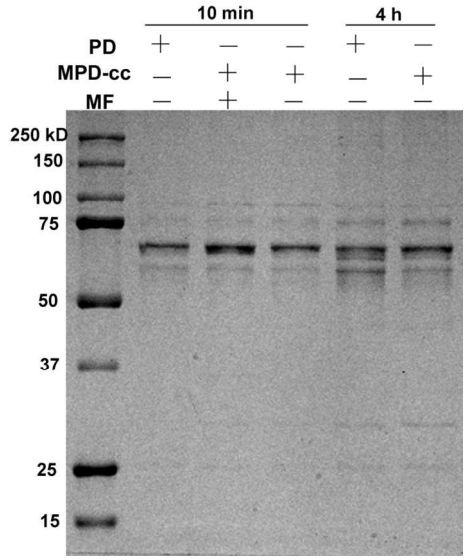

Fig. 3 SDS-polyacrylamide gel electrophoresis (SDS-PAGE) of protein corona of PD and MPD-cc complexes after 10-min or 4-h incubation in the presence of serum. 120 mT magnetic field was applied in MPD-cc complexes for 10 min. The molecular weights of the proteins in marker were reported on the left for reference.

solubility, and consequently affect the nature of nanoparticle biomolecule corona[32, 35].

3.4 Cell membrane wounding assay based on the impedance measurement

After protein corona formation, gene complexes undergo interaction with cell membrane. It was reported that some high efficiency transfection systems were associated with the cell membrane wounding, which would incur severe cytotoxicity[36]. Electrochemical impedance measurement has proven a simple and effective method for real-time monitoring of cell integrity or cell adhesion[20, 21, 36]. Once the cell membrane was destroyed, the impedance of cell monolayer would decrease as a result. Thus, the changes of cell membrane impedance are also considered as an index of cell viability[20, 36]. In the present study, since the impedance magnitude changes of each experiment group treated with gene complexes were similar at 4 h and 24 h, the latter time point was selected for

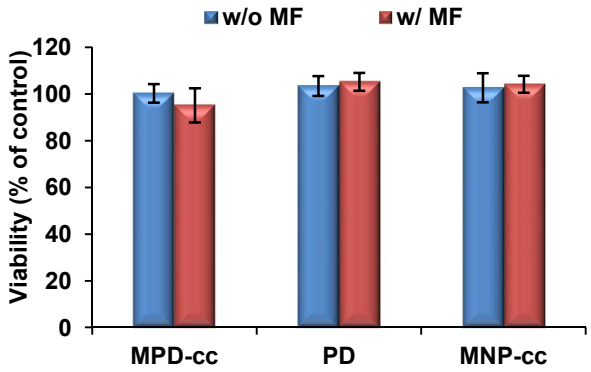

Fig. 4 Cell viability calculated from electrochemical impedance spectroscopy (EIS) measurements (24 h). 120 mT magnetic field was applied in magnetofection. Viability (%) was obtained by the relative impedance values of transfected cells against control experiment. All data were shown as mean ± S.D. (n = 5).

calculation of the relative cell viability against the control group (Fig. 4). It was obviously that the cells treated with PD and MPD-cc complexes showed high cell viability (~ 100%), indicating almost no cell membrane wounding took place[37]. The results were also consistent with our previous cytotocixity study by MTT assays for the NAD(P)H-dependent cellular oxidoreductase enzymes activity measurement[10].

3.5 Interaction of gene complexes with cells post incubation

Cellular uptake of gene complexes was essential step for gene transfection, involving cellular association and internalization. Thus flow cytometry was used to explore the interaction of gene complexes with cells under various incubation modes in the presence of serum (Fig. 5).

No difference in cellular uptake was detected between the cells treated with PD and MPD-cc complexes in the absence of magnetic field for 10 min showing about 40% of FITC-positive cells and similar mean fluorescence intensity (Fig. 5A and B). While for the cells incubated with fluorescent MPD-cc complexes as magnetofection mode (MPD-cc + MF, 10 min), the percentage of fluorescent positive cells sharply increased to 80%, along with at least 2-fold increase in mean fluorescent intensity than that of PD group. It indicated that MPD-cc complexes were able to interact with most of the cells in 10 min in magnetofection, and the application of a magnetic field had considerable effect on sedimentation of particles on the cells[10]. At 4-h time point, positive cells in PD group also reached 80% of the total population, but the mean fluorescence intensity was much lower than that in magnetofection. The results were consistent with the phenomena in protein corona evaluation, in which more protein adsorption would inhibit cellular uptake of gene complexes. The fluorescence intensity difference of magnetofection between 10 min and 10 min + W + 4 h incubation models might be due to the loss of some loosely associated complexes during the trypsin treatment[38].

The internalization of various complexes was evaluated after adding trypan blue, a cell membrane-impermeable dye which cannot quench the fluorescence of magnetic complexes inside cells[17] (Fig. 5C and D). With 10 min incubation, only few cells (4%) internalized FITC labeled PD complexes, corresponding to about one tenth of the total cell uptake (Fig. 5B). While in the magnetofection conditions, fluorescent-positive cells reached 20%, which was one fourth of total cell uptake (80%, Fig. 5B). Meanwhile the mean fluorescence intensity in magnetofection was about 6-fold higher than that of PD complexes. This efficient and fast internalization of gene complexes under magnetic field was also confirmed by the cell membrane capacitance deduced from the impedance spectra (Fig. S3). It showed a sharp drop during the first few minutes in magnetofection, revealing the reduced membrane surface area due to cellular internalization[39]. When the incubation time was prolonged to 4 h, the percentage of cellular internalization was increased up to ~ 70% in magnetofection, similar to the traditional process (PD, 4 h). But significant difference was found in the mean fluorescence intensity. Cells incubated with the PD or MPD-cc complexes without magnetic field showed only about one fourth of fluorescence intensity of that treated with MPD-cc + MF, indicating less PD complexes were located inside the positive cells[40].

3.6 Intracellular behavior of gene complexes

Besides overcoming the barriers of cell membranes, efficient endosomal escape and nuclear import of cargo DNA are also vital for the successful gene transfection[41]. The intracellular fate of gene complexes was thus visualized by confocal microscopy (Fig. 6). Double-labeled gene complexes showed yellow color as a result of overlaid colors from Cy5 labeled pGL3 (red) and FITC labeled PEI (green). At 4-h incubation time, the white color clusters were obviously observed (as indicated by white arrows) in the cells treated with PD (or MPD-cc complexes without magnetic field), reflecting a colocalization of PEI and DNA in the lysosomal compartment (Fig. 6A). In contrast, there was little such white cluster in the cells incubated as magnetofection process. 24 h later, when most PD complexes were trapped in the blue fluorescent lysosomes, MPD-cc complexes in magnetofection were mainly yellow in color and some turned red (orange arrows), indicating successful endosomal escape and incomplete overlap of PEI and DNA[42]. As the staining of endosomes/lysosomes by fluorescent tracker is known to depend upon the acidity of the endosomal/lysosomal compartments, in the case of (MPD-cc + MF), the attenuated weak blue fluorescence at 24 h time point suggested the destruction of the acid compartment environment, which might be one of the reasons for efficient endosomal/lysosomal escape and benefit for the gene protection[42]. More importantly, the red dots resulting from the complexes dissociation seemed to localize in the position of nucleus (as indicated by red arrows, Fig. 6A). For better distinction, cell nuclei were labeled with DAPI (blue) at 24 h post incubation (Fig. 6B). It was obvious that some dots in the cells treated with magnetofection were exactly localized in the nucleus (white arrows) and the complexes in PD and MPD-cc without magnetic field distributed around nucleus (yellow arrows).

As the difference in assembly sequence, size, surface property and charge of magnetic or nano-sized vectors could affect the adsorbed proteins (protein corona) and the intracellular process and location[18, 26, 32, 35], the diverse surface properties and protein corona from adding of negatively charged magnetic particles (MNP-cc) and shorter incubation time (10 min) might exert verified effects on the interaction between particles and cells. Above results (Fig. 4-6) may well explain the better transfection performance of magnetofection compared with traditional PD complexes in the presence of serum, supporting the notion that protein corona formation is critical for the gene delivery[34, 43], which could sequentially affect the following

steps in cellular uptake, endosome escape and nuclear import[44]. The improved transfection may result from less protein adsorption, more and efficient gene delivery (Scheme 1).

3.7 *In vivo* and *ex vivo* imaging of mice administrated with gene complexes

Biodistribution is very important for the transfection efficiency *in vivo*, so the accumulation of fluorescently labeled gene complexes in tumor bearing mice was evaluated after intravenous injection. As the cationic gene complexes could rapidly distribute in targeting site and main organs after 15 min post administration[45, 46], the fluorescent images were taken at 8 h time point in our study by near-infrared fluorescent (NIRF) signal observation (Fig. 7). From the images, much stronger signal of Cy5 was detected at tumor area in the magnetofection group compared with that in PD complexes (Fig. 7A). The strongest signal from liver might be attributed to the rapid clearance of nanoparticles by the mononuclear phagocytic system[34, 47].

Considering the permeation of fluorescence from body, fluorescent images of tumor and main organs including heart, liver,

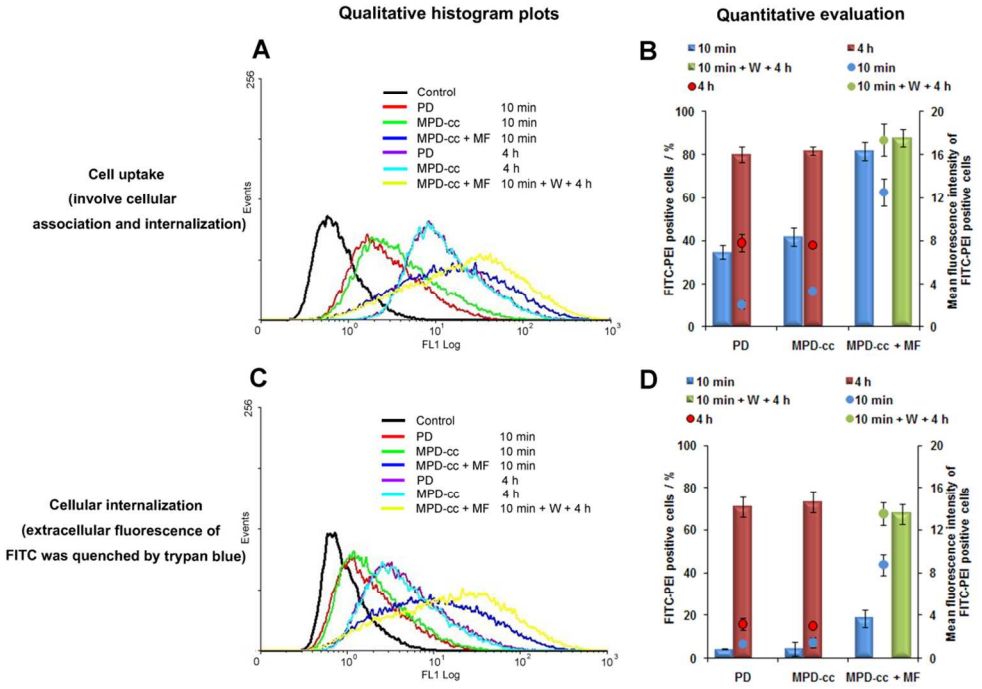

Fig. 5 Flow cytometry assays of HepG2 cells incubated with fluorescent gene complexes in the presence of serum. PEI was labeled with FITC for cellular uptake evaluation (involving cellular association and internalization, A and B), and the extracellular fluorescence of FITC was quenched by trypan blue for internalization measurement (C and D). Bar graphs showed percentage of the FITC-positive cells, and the dot graphs indicated mean intensity of FITC-positive cells (B and D). Three kinds of incubation modes with gene complexes were used: (Ⅰ) 10 min incubation, (Ⅱ) 4 h incubation, (Ⅲ) 10 min incubation, washing with cold PBS and another 4 h incubation with fresh culture medium (10 min + W + 4 h). 120 mT magnetic field was applied for the 10-min incubation in magnetofection (MPD-cc + MF). All the data were shown as mean ± S.D. (n = 5).

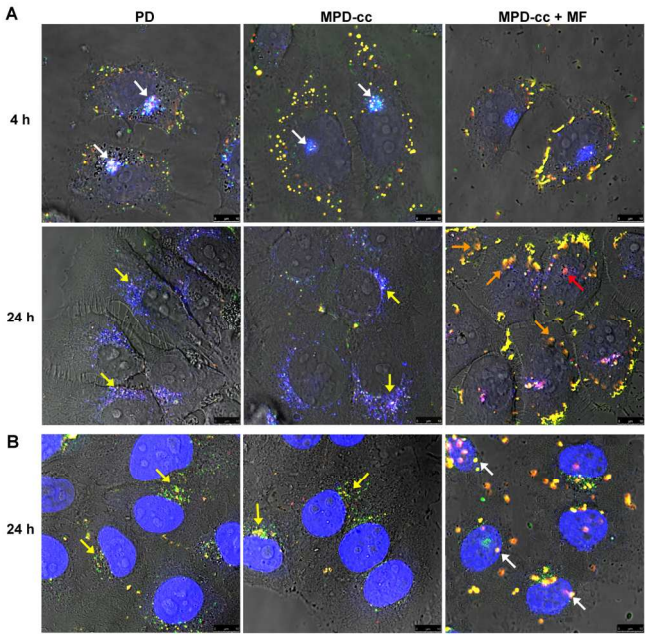

Fig. 6 Intracellular fate of gene complexes in HepG2 cells after incubation as traditional transfection or magnetofection process in the presence of serum. (A) Tracing of endosomal escape of gene complexes (yellow) containing FITC labeled PEI (green) and Cy5 labeled DNA (red) in cells with lysoTracker™ DND-22 labeled lysosomes (blue) at two different time points (4 and 24 h). White color indicated the occasions of coincidence between the complexes and the lysosomes (as indicated by white arrows). Traditional transfection was performed with 4-h incubation. 120 mT magnetic field was applied for 10 min in magnetofection (MPD-cc + MF). (B) Tracing of nuclear entry of complexes (as indicated by white arrows) by FITC labeled PEI, Cy5 labeled DNA in cells with DAPI labeled nucleus (blue) at 24-h time point. (scale bar = 10 μm).

spleen, lung and kidney were dissected for *ex vivo* evaluation (Fig. 7B). The fluorescent images were acquired with the same exposure time for the same tissue in different groups, while the exposure time for each tissue was different. The fluorescent signal in tumor was much stronger in magnetofection group than PD complexes group, indicating magnetofection could effectively target to tumor, which is probably a major reason of the effective transfection *in vivo* by magnetofection (Fig. 8). There was no significant signal difference in liver, lung and kidney between the two groups relatively, while lower fluorescence intensity was found in heart and spleen in magnetofection group. These results demonstrated that magnetofection not only realized the magnetic targeting, but also decreased the accumulation of complexes at non-targeting site, which would probably reduce the unexpected toxicity to normal organs. The particles accumulated in liver and kidney were due to the hepatic clearance and urine excretion[47], and the lung accumulation was resulted from some aggregates formation in the lung[46, 48].

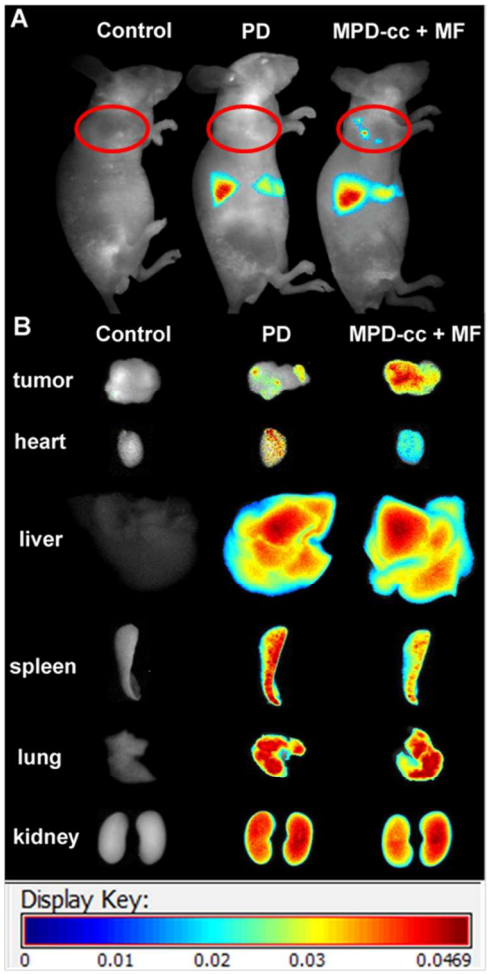

Fig. 7 *In vivo* fluorescence imaging of tumor-bearing mice after systemic administration of PD and MPD complexes for 8 h. (A) Images of the right side of live mice, (B) Images of the dissected tissues of mice. DNA was labeled by Cy5. 400 mT magnetic field was applied in magnetofection group (MPD-cc + MF). Fe to DNA weight ratio in MPD-cc complexes was equal to 0.8. Control group was administrated with 5% w/v glucose solution.

3.8 Gene expression *in vivo*

Intravenous injection is efficient administration for nucleic acid delivery to distant organs and tumors, but still encounters many challenges[3, 48]. Besides the quick opsonization of cationic nanoparticles and fast degradation of DNA in systemic circulation, the extremely low plasma concentration of DNA[49] seriously reduces the DNA concentration at target site. Thus it requires optimized targeting properties and stricter size control of carriers for tumor-specific accumulation[50]. In our previous study, low aggregated magnetic polyethyleneimine complexes with high saturation magnetization (MPD-cc) were designed for magnetofection, showing high transfection efficiency by intratumor injection[10]. Now, we proceeded the estimation in systemic administration. As expected, there were different levels of luciferase expression in the tumor between magnetofection and traditional transfection groups (Fig. 8). Transfection by MPD-cc complexes under a magnetic field produced the highest level of luciferase activity, which was approximately 5-fold higher than that of the PD complexes ($p < 0.05$). Such improvement demonstrated that MPD-cc complexes with small size possessed enough magnetic response, even in complicated body conditions. And the magnetofection was able to deliver more DNA to the tumor for gene expression after intravenous administration, supporting the high targeting ability of magnetofection reported by previous studies[51]. No significant difference was found in the case of PD and MPD-cc complexes without magnetic field, both showing relatively low levels of luciferase activity in the tumor. Among the normal tissues, lung showed relatively higher gene expression, while liver with more gene capture (Fig. 7A) displayed negligible transfection than the control. Similar observations were found in other cationic gene vectors studies[45, 46, 52]. The possible explanation might be that the positively charged polyplexes would form aggregates in the lung which induce backpressure in the blood flow and in turn push the particles through the lung endothelium into lung cells[46, 48]. While the polyplexes accumulated in the liver might be inactivated by metabolism. Moreover, it is also a common phenomenon that the complexes distribution pattern did not match the luciferase gene expression pattern because *in vivo* gene expression would encounter barriers like passage through blood

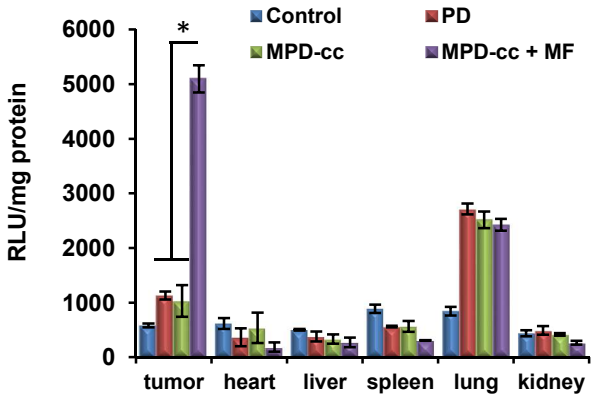

Fig. 8 *In vivo* luciferase activity in tumor and organs after intravenous treatment of gene complexes 48 h. 400 mT magnetic field was applied in magnetofection group (MPD-cc + MF). Fe to DNA weight ratio in MPD-cc complexes was 0.8. Control group was administrated with 5% w/v glucose solution. ($n = 6$, $^*p < 0.05$).

capillary, diffusion through tissues and entrance into cells, and the transfection ability of different kinds of cells is distinctive[3, 10, 19, 47].

4 Conclusions

The low aggregated magnetic polyethyleneimine/DNA (MPD-cc) complexes were constructed to realize serum resistance transfection *in vitro*, and the present study aimed at the mechanism elucidation and investigation on possible *in vivo* application of MPD-cc through systemic administration. In the presence of serum, the sizes of cationic gene complexes increased, but there was no large-size aggregation. Zeta potentials of all complexes switched to negative value due to adsorption of anionic serum protein. No cellular membrane wounding was found after incubation with any kinds of gene carriers. The MPD-cc complexes in magnetofection condition showed much faster and more interaction with cells not only in the cellular uptake step but also in the internalization process, partly due to less unexpected protein adsorption. Furthermore, the intracellular fate study revealed that only MPD-cc complexes with extra magnetic field application could effectively realize endosomal escape and nucleus location. *In vivo* studies demonstrated effective magnetofection of MPD-cc complexes after intravenous administration, largely due to the improved distribution of gene complexes. These works would contribute to further exploration of the serum resistance strategy for gene delivery and expand the potential application of magnetic targeting to hard-to-reach tissues and organs via systemic delivery. Until now, no reports have revealed the clear mechanism of how the magnetic force or magnetic particles plays so important role in the intracellular process (eg. endosomal escape and nuclear import), as well as the status of magnetic particles in the bloodstream. Thus more details about the protein corona analysis and hydrodynamic evaluation of vectors in the blood are designed for our further work.

Acknowledgements

This study was supported by National Natural Science Foundation of China (NSFC, No. 51133004, 81361140343，31271020), National Basic Research Program of China (National 973 programs, No. 2011CB606206), Fund from Sino-German Center for Research Promotion (GZ 756), European Commission Research and Innovation (PIRSES-GA-2011-295218), Fund from Science and Technology Department of Sichuan Province (2013FZ0003), Research Fund for the Doctoral Program of Higher Education of China (Grant No. 20100181120075), and the Excellent Young Scholar Program of Sichuan University (2011SCU04A14). The authors also thank Prof. Zhanwen Xiao for kind help in the electrochemical impedance measurement and Dr. Hongmei Song for the kind help to polish the English expression.

Notes and references

National Engineering Research Center for Biomaterials, Sichuan University, Chengdu 610064, P. R. China. E-mail: zwgu@scu.edu.cn; nie_yu@scu.edu.cn
* Corresponding authors: Zhongwei Gu and Yu Nie
†Electronic Supplementary Information (ESI) available: Figure of the cell-device system in impedance measurement, images of pEGFP gene expression, and membrane capacitance. See DOI: 10.1039/b000000x/

1. E. Wagner and J. Kloeckner, in Polymer Therapeutics I, eds. R. Satchi-Fainaro and R. Duncan, Springer Berlin Heidelberg2006, vol. 192, ch. 23, pp. 135-173.
2. A. L. Capriotti, G. Caracciolo, G. Caruso, P. Foglia, D. Pozzi, R. Samperi and A. Lagana, Proteomics, 2011, 11, 3349-3358.
3. R. Kircheis, L. Wightman and E. Wagner, Advanced Drug Delivery Reviews, 2001, 53, 341-358.
4. Y. He, G. Cheng, L. Xie, Y. Nie, B. He and Z. Gu, Biomaterials, 2013, 34, 1235-1245.
5. M. Ogris, S. Brunner, S. Schuller, R. Kircheis and E. Wagner, Gene Ther, 1999, 6, 595-605.
6. N. Hauptmann, M. Pion, M. A. Munoz-Fernandez, H. Komber, C. Werner, B. Voit and D. Appelhans, Macromolecular bioscience, 2013, 13, 531-538.
7. F. Scherer, M. Anton, U. Schillinger, J. Henke, C. Bergemann, A. Kruger, B. Gansbacher and C. Plank, Gene Ther, 2002, 9, 102-109.
8. X. Pan, J. Guan, J. W. Yoo, A. J. Epstein, L. J. Lee and R. J. Lee, Int J Pharm, 2008, 358, 263-270.
9. S.-L. Sun, Y.-L. Lo, H.-Y. Chen and L.-F. Wang, Langmuir, 2012, 28, 3542-3552.
10. L. Xie, W. Jiang, Y. Nie, Y. He, Q. Jiang, F. Lan, Y. Wu and Z. Gu, RSC Advances, 2013, 3, 23571-23581.
11. F. Krotz, C. de Wit, H. Y. Sohn, S. Zahler, T. Gloe, U. Pohl and C. Plank, Mol Ther, 2003, 7, 700-710.
12. A. K. Gupta and M. Gupta, Biomaterials, 2005, 26, 3995-4021.
13. X. Wang, L. Zhou, Y. Ma, X. Li and H. Gu, Nano Research, 2010, 2, 365-372.
14. B. Steitz, H. Hofmann, S. W. Kamau, P. O. Hassa, M. O. Hottiger, B. von Rechenberg, M. Hofmann-Amtenbrink and A. Petri-Fink, Journal of Magnetism and Magnetic Materials, 2007, 311, 300-305.
15. F. M. Kievit, O. Veiseh, N. Bhattarai, C. Fang, J. W. Gunn, D. Lee, R. G. Ellenbogen, J. M. Olson and M. Zhang, Advanced functional materials, 2009, 19, 2244-2251.
16. S. Huth, J. Lausier, S. W. Gersting, C. Rudolph, C. Plank, U. Welsch and J. Rosenecker, J Gene Med, 2004, 6, 923-936.
17. A. M. Sauer, K. G. de Bruin, N. Ruthardt, O. Mykhaylyk, C. Plank and C. Brauchle, J Control Release, 2009, 137, 136-145.
18. M. Arsianti, M. Lim, C. P. Marquis and R. Amal, Biomacromolecules, 2010, 11, 2521-2531.
19. S. Prijic, L. Prosen, M. Cemazar, J. Scancar, R. Romih, J. Lavrencak, V. B. Bregar, A. Coer, M. Krzan, A. Znidarsic and G. Sersa, Biomaterials, 2012, 33, 4379-4391.
20. J. H. Yeon and J.-K. Park, Analytical Biochemistry, 2005, 341, 308-315.
21. R. Meissner, B. Eker, H. Kasi, A. Bertsch and P. Renaud, Lab on a chip, 2011, 11, 2352-2361.
22. P. Kurzweil and H. J. Fischle, Journal of Power Sources, 2004, 127, 331-340.
23. A. Saovapakhiran, A. D'Emanuele, D. Attwood and J. Penny, Bioconjug Chem, 2009, 20, 693-701.
24. S. Son and W. J. Kim, Biomaterials, 2010, 31, 133-143.
25. I. Lynch, A. Salvati and K. A. Dawson, Nat Nano, 2009, 4, 546-547.
26. M. Arsianti, M. Lim, C. P. Marquis and R. Amal, Langmuir, 2010, 26, 7314-7326.
27. S. Li, W. C. Tseng, D. B. Stolz, S. P. Wu, S. C. Watkins and L. Huang, Gene Ther, 1999, 6, 585-594.
28. K. Wong, G. Sun, X. Zhang, H. Dai, Y. Liu, C. He and K. W. Leong, Bioconjug Chem, 2006, 17, 152-158.
29. A. L. Capriotti, G. Caracciolo, G. Caruso, P. Foglia, D. Pozzi, R. Samperi and A. Lagana, Anal Biochem, 2011, 419, 180-189.
30. D. E. Owens, 3rd and N. A. Peppas, Int J Pharm, 2006, 307, 93-102.
31. M. S. Ehrenberg, A. E. Friedman, J. N. Finkelstein, G. Oberdorster and J. L. McGrath, Biomaterials, 2009, 30, 603-610.
32. M. P. Monopoli, D. Walczyk, A. Campbell, G. Elia, I. Lynch, F. B. Bombelli and K. A. Dawson, J Am Chem Soc, 2011, 133, 2525-2534.
33. H. Faneca, S. Simoes and M. C. Pedroso de Lima, J Gene Med, 2004, 6, 681-692.
34. S. Nagayama, K. Ogawara, Y. Fukuoka, K. Higaki and T. Kimura, Int J Pharm, 2007, 342, 215-221.

35. M. Lundqvist, J. Stigler, G. Elia, I. Lynch, T. Cedervall and K. A. Dawson, Proceedings of the National Academy of Sciences of the United States of America, 2008, 105, 14265-14270.
36. L. Ceriotti, J. Ponti, F. Broggi, A. Kob, S. Drechsler, E. Thedinga, P. Colpo, E. Sabbioni, R. Ehret and F. Rossi, Sensors and Actuators B: Chemical, 2007, 123, 769-778.
37. D. Ang, Q. V. Nguyen, S. Kayal, P. R. Preiser, R. S. Rawat and R. V. Ramanujan, Acta Biomater, 2011, 7, 1319-1326.
38. S.-F. Peng, M.-J. Yang, C.-J. Su, H.-L. Chen, P.-W. Lee, M.-C. Wei and H.-W. Sung, Biomaterials, 2009, 30, 1797-1808.
39. K. O. Holevinsky and D. J. Nelson, Biophysical Journal, 1998, 75, 2577-2586.
40. Y. Yue, F. Jin, R. Deng, J. Cai, Y. Chen, M. C. M. Lin, H.-F. Kung and C. Wu, Journal of Controlled Release, 2011, 155, 67-76.
41. Y. Nie, M. Günther, Z. Gu and E. Wagner, Biomaterials, 2011, 32, 858-869.
42. Y. He, Y. Nie, L. Xie, H. Song and Z. Gu, Biomaterials, 2014, 35, 1657-1666.
43. G. Caracciolo, L. Callipo, S. C. De Sanctis, C. Cavaliere, D. Pozzi and A. Lagana, Biochimica et biophysica acta, 2010, 1798, 536-543.
44. S. Simões, V. Slepushkin, P. Pires, R. Gaspar, M. C. Pedroso de Lima and N. Düzgüneş, Biochimica et Biophysica Acta (BBA) - Biomembranes, 2000, 1463, 459-469.
45. A. Zintchenko, A. S. Susha, M. Concia, J. Feldmann, E. Wagner, A. L. Rogach and M. Ogris, Mol Ther, 2009, 17, 1849-1856.
46. G. Navarro, G. Maiwald, R. Haase, A. L. Rogach, E. Wagner, C. T. de Ilarduya and M. Ogris, J Control Release, 2010, 146, 99-105.
47. K. Kunath, A. von Harpe, D. Fischer, H. Petersen, U. Bickel, K. Voigt and T. Kissel, Journal of Controlled Release, 2003, 89, 113-125.
48. E. Wagner, Pharmaceutical research, 2004, 21, 8-14.
49. B. Chertok, A. E. David, B. A. Moffat and V. C. Yang, Biomaterials, 2009, 30, 6780-6787.
50. M. Nishikawa and L. Huang, Human gene therapy, 2001, 12, 861-870.
51. L. Han, A. Zhang, H. Wang, P. Pu, C. Kang and J. Chang, Journal of Applied Polymer Science, 2011, 121, 3446-3454.
52. R. Kircheis, S. Schuller, S. Brunner, M. Ogris, K. H. Heider, W. Zauner and E. Wagner, J Gene Med, 1999, 1, 111-120.